Separation and Purification Technology 171 (2016) 118–122

Contents lists available at ScienceDirect

Separation and Purification Technology

journal homepage: www.elsevier.com/locate/seppur

Improved photocatalytic activity of TiO_2 modified with unique O–Zn–Cl surface species

Sai Yan [a], Yanlong Yu [b,*], Yao Gu [a], Yue Liu [c], Yaan Cao [a]

[a] MOE Key Laboratory of Weak-Light Nonlinear Photonics, Ministry of Education, TEDA Applied Physics Institute and School of Physics, Nankai University, Tianjin 300457, China
[b] Department of Materials Chemistry, College of Chemistry, Nankai University, Tianjin 300457, China
[c] College of Material Science & Engineer, Liaoning Technology University, Fuxin 123000, China

ARTICLE INFO

Article history:
Received 16 November 2015
Received in revised form 15 March 2016
Accepted 16 July 2016
Available online 18 July 2016

Keywords:
TiO_2
O–Zn–Cl surface species
Photo-reduction of CO_2
Surface modification

ABSTRACT

TiO_2 modified with unique surface O–Zn–Cl species is prepared by a simple sol-gel method. The Zn modified TiO_2 samples exhibit improved photocatalytic activity on photo-reduction of CO_2 into CH_4, compared with pure TiO_2. The surface structure and photocatalytic properties are investigated by Raman, XRD, XPS, UV–vis absorption spectra, PL and time-resolved PL decay curves techniques. It is revealed that the existence of O–Zn–Cl species can extend the absorption into visible region, inhibit the recombination of charge carriers and prolong the lifetime of photogenerated electrons. Therefore the O–Zn–Cl modified TiO_2 samples represent an improved photocatalytic performance on photo-reduction of CO_2 into CH_4.

1. Introduction

Titanium Dioxide is usually regarded as one of the most promising opti-electrical functional materials, which can be applied in many fields, such as photocatalysis and photosynthesis [1–5]. Huge efforts have been devoted to improve the photocatalytic performance of TiO_2, for example doping with metal or non-metal elements [6–11], composition with other semiconductors [12–15] and surface modification [16–21]. Among these proposes, the introduction of Zn species into TiO_2 system by doping, composition or modification has been investigated by many researchers. Wang and his co-workers develop a method to introduce Zn submitting for Ti in TiO_2 film with enhanced energy conversion efficiency in dye sensitized solar cells [22]. Xu et al. prepared Zn surface doped TiO_2 nanotubes with enhanced photocatalytic activity on photodegradation of methyl orange [23]. Li et al. investigate the ZnO composited with B doped TiO_2 with enhanced visible photocatalytic activity [24]. Recently, we found a new kind of species, O–Zn–Cl species, formed on the surface of TiO_2 when the calcination temperature is below 500 °C and the dopant content is below 5% [25]. However, the influence of the surface O–Zn–Cl species on the band structure, opti-electrical properties and the photocatalytic performance of TiO_2 is still unknown. Moreover, modifying TiO_2 with surface species is usually considered as an efficient technique to enhance the photocatalytic performance by creating a new surface energy level, extending response into visible region and suppressing the recombination of charge carriers [16–21]. Our previous work has demonstrated the unique O–Me–Cl_x (Me = In, Ni or Pd) surface species modified on the surface of TiO_2 can increase the absorption in visible region, promote the separation of charge carriers and enhance the photocatalytic activity. It is expected the TiO_2 modified with O–Zn–Cl species would act as the same role to improve the photocatalytic activity of the photocatalytic under visible irradiation.

Herein, the Zn modified TiO_2 is prepared by a simple sol-gel method and exhibits enhanced photocatalytic on photo-reduction of CO_2 with H_2O into CH_4. Owing to the surface energy level of O–Zn–Cl species, the visible response is enhanced and the photogenerated electrons and holes are separated effectively, improving the photocatalytic activity. The band structure, behaviors of the charge carriers as well as the photocatalytic mechanism are also studied in details.

2. Experimental details

2.1. Catalyst preparation

All chemicals used were of analytical grade and the water was deionized water (>18.2 MΩ cm). At room temperature, certain amount of $Zn(NO_3)_2$ were dissolved into 40 mL of ethanol. After mixing for half an hour, 1 mL HCl solution (12 mol/L) and 12 mL

* Corresponding author.
E-mail addresses: yanlong.yu@qq.com (Y. Yu), caoya@nankai.edu.cn (Y. Cao).

http://dx.doi.org/10.1016/j.seppur.2016.07.022
1383-5866/

of $Ti(OC_4H_9)_4$ was added dropwise into the mixture under vigous stirring. Then 1 mL of deionized water was added for further hydrolysis. The pH value of the mixture is evaluated to be 0.5. The mixture was stirred until the formation of TiO_2 gel. After aging for 24 h, the TiO_2 gels were dried at 100 °C for 10 h and annealed at 450 °C in a muffle for 150 min. The obtained sample was donated as TiO_2-Zn, where the molar ratio of Zn to Ti (Zn/Ti) is 5%. Pure TiO_2 is also synthesized, just without the addition of $Zn(NO_3)_2$.

2.2. Characterization

Raman spectra were taken on a Renishaw inVia Raman microscope by using the 785 nm line of a Renishaw HPNIR 785 semiconductor laser. X-ray diffraction (XRD) patterns were acquired on a Rigaku D/max 2500 X-ray diffraction spectrometer (Cu Ka, λ = 1.54056 Å) at a scan rate of 0.02° 2θ s^{-1}. The average crystal size was calculated using the Scherrer equation ($D = k\lambda/Bcos\theta$). After degassing at 180 °C, the BET surface area was determined via the measurement of nitrogen adsorption–desorption isotherms at 77 K (Micromeritics Automatic Surface Area Analyzer Gemini 2360, Shimadzu). X-ray photoelectron spectroscopy (XPS) measurements were carried out with an ESCA Lab 220i-XL spectrometer by using an unmonochromated Al Ka X-ray source (148.6 eV). All spectra were calibrated using the binding energy (BE) of the adventitious C1s peak at 284.6 eV. Diffuse reflectance UV–vis absorption spectra (UV–vis DRS) were collected with a UV–vis spectrometer (U-4100, Hitachi). Photoluminescence (PL) spectra were acquired by using the 325 nm line of a nano-second Nd: YAG laser (NL303G) as excitation source. The experimental setup consists of a spectrometer (Spex 1702), a photomultiplier tube (PMT, Hamamatsu R943), a lock-in amplifier, and a computer for data processing. All of the measurements were carried out at room temperature (25 ± 2 °C).

2.3. Evaluation of photo-reduction activity

The photo-reduction activity of the photocatalysts was evaluated by photo-reduction of CO_2 and H_2O into CH_4. 150 mg of photocatalyst was uniformly dispersed on a glass sheet with an area of 9.4 cm^2. A 500 W spherical Xenon arc lamp (Philips, Belgium, 35 mW/cm^2, 290–800 nm) was used as the light source of photocatalytic reaction. The glass sheet was placed at the bottom of a sealed Pyrex glass reaction vessel (410 mL) which is located 10 cm away from the light source and vertical to the light beam. Prior to the illumination, the high purity of CO_2 gas (99.99%), via a flow controller, was followed into the reaction setup for 45 min for reaching ambient pressure. Then the reaction vessel was sealed and 2 mL of deionized water was injected into the reaction system as reducer. During irradiation, about 0.4 mL of gas was continually taken from the reaction cell every 2 h for subsequent CH_4 and CO concentration analysis by using a gas chromatograph (Techcomp GC-7890F, equipped with a 1 m × ϕ3 mm TDX-01 packed column and a flame ionization detector (FID)). N_2 was used as the carrier gas. Since FID cannot detect CO and CO_2, an additional converter (Techcomp converter loaded with Ni catalyst) was attached to the GC system between the column and detector, which can reduce CO to methanol ($CO + H_2 \rightarrow CH_4OH$) and CO_2 to methane ($CO_2 + 4H_2 \rightarrow CH_4 + 2H_2O$). Hence, CO and CO_2 could be analyzed simultaneously.

3. Results

To investigate the surface structure of the Zn modified TiO_2 samples, Raman spectra of TiO_2 and TiO_2-Zn are plotted in Fig. 1. Both the TiO_2 and TiO_2-Zn samples show the typical characteristic bands at about 142 cm^{-1}, 195 cm^{-1}, 395 cm^{-1}, 515 cm^{-1} and 637 cm^{-1}, attributed to the E_g, B_{1g}, A_{1g}, B_{2g} and E_g vibrational modes of anatase [7], respectively. In comparison with pure TiO_2, some new weak Raman peaks at about 256 cm^{-1}, 333 cm^{-1} and 450 cm^{-1} are observed for TiO_2-Zn sample. The Raman peaks at about 333 cm^{-1} and 450 cm^{-1} are ascribed to the E_2 mode of ZnO. The Raman peak at about 256 cm^{-1} is the same as that for $ZnCl_2$ (inset of Fig. 1). These Raman spectra demonstrate the existence of Zn–O bonds and Zn–Cl bonds, indicating the introduced Zn^{2+} ions link with O and Cl simultaneously to form O–Zn–Cl species. To further demonstrate the existence of O–Zn–Cl species, XRD and XPS are carried out in the following sections.

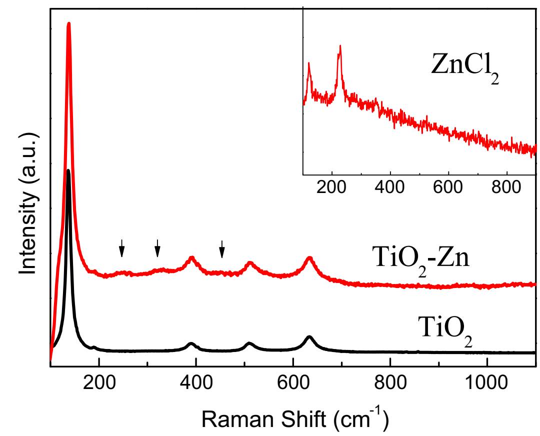

Fig. 1. Raman spectra of TiO_2 and TiO_2-Zn. Inset shows the Raman spectrum of $ZnCl_2$.

The XRD spectra of pure TiO_2 and TiO_2-Zn are shown in Fig. 2. It is obvious that only the characteristic peaks of anatase TiO_2 are observable and no other phase such as rutile are detected, suggesting anatase is the only phase for TiO_2 and TiO_2-Zn. It is known that the ionic radius of Zn^{2+} ions is larger than that for Ti^{4+} ions (Zn^{2+}: 74 pm, Ti^{4+}: 68 pm). An increase of lattice parameters and cell volume is expected if Zn^{2+} ions substitute the lattice Ti^{4+} ions. However, it is found from the inset of Fig. 2 that the peak position of (1 0 1) plane remain almost unchanged and the lattice parameters as well as the cell volume is almost the same (Table 1) [26], compared with TiO_2. Hence it can be concluded that the introduced Zn^{2+} are not doped into TiO_2 lattice in substitutional mode, implying that the introduced Zn^{2+} ions exist as surface O–Zn–Cl species.

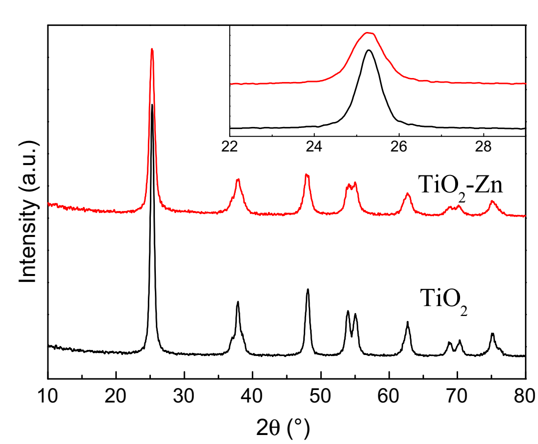

Fig. 2. XRD spectra of pure TiO_2 and TiO_2-Zn. Inset shows the enlargement of (1 0 1) plane for anatase.

Table 1
Lattice parameters, cell volume, crystal size and specific surface areas of the TiO_2 and TiO_2-Zn.

Samples	Lattice parameter (Å)			Cell volume ($Å^3$)	Crystal size (nm)	S_{BET} ($m^2\ g^{-1}$)
	a	b	c			
TiO_2	3.7857	3.7857	9.5118	136.32	12.4	56.9353
TiO_2-Zn	3.7876	3.7876	9.4963	136.23	8.9	63.4306

To further investigate the chemical states of the introduced Zn^{2+} ions, XPS analysis is carried out. As shown in Fig. 3A, the Cl 2p spectrum of TiO_2 could be deconvolved into two peaks, ascribed to the Cl $2p_{3/2}$ and Cl $2p_{1/2}$, respectively. The peak of Cl $2p_{3/2}$ located at about 198.1 eV is ascribed to the surface O–Ti–Cl structure, which shows no response to visible region and have no influence on the visible photocatalytic activity [17]. For the TiO_2-Zn samples, the peak intensity of Cl 2p spectrum increased significantly, compared with pure TiO_2, suggesting more chlorine related species formed on the surface of TiO_2. The peak of Cl $2p_{3/2}$ located at about 199.1 eV, between that for $TiCl_4$ (198.2 eV) and $ZnCl_2$ (199.7 eV) [26], indicating the Cl^- ions are linked with the Zn^{2+} ions. Moreover, it is found from Fig. 3B that the Zn $2p_{3/2}$ peak for TiO_2-Zn at about 1022.1 eV is between ZnO (1021.9 eV) and $ZnCl_2$ (1022.5 eV), suggesting the introduced Zn^{2+} ions are linked with unsaturated O^{2-} ions and Cl^- ions simultaneously. Moreover, it is found from the XPS that the atom percentage of Zn and Cl for TiO_2-Zn samples is 4.53% and 4.99%, respectively. These XPS results further demonstrated that the Zn^{2+} ions are linked with the surface unsaturated O^{2-} ions and Cl^- ions simultaneously to form O–Zn–Cl species on the surface of TiO_2, while some other Cl^- ions are linked with the surface unsaturated Ti to form the surface O–Ti–Cl structure. These XPS results are in good agreements with the discussion above.

To investigate the influence of surface O–Zn–Cl species on the band structure of TiO_2, UV–vis absorption spectra TiO_2 and TiO_2-Zn are plotted in Fig. 4. The TiO_2 based samples exhibit strong absorption around 340 nm, attributed to the band-to-band transition of anatase. The band threshold is estimated to be 405 nm, corresponding to a band gap of 3.06 eV. The absorption peak attributed to the band-to-band transition for TiO_2-Zn sample is almost the same as that for pure TiO_2. Moreover, there is a new absorption peak from 400 nm to 600 nm found for TiO_2-Zn. The absorption maximum is at about 430 nm, corresponding to an energy gap of 2.88 eV, suggesting the energy level of surface O–Zn–Cl species locates at about 0.2 eV below the conduction band of TiO_2. Therefore, the enhanced absorption in visible region can be attributed to the electron transition from the valence band of TiO_2 to the surface energy level of O–Zn–Cl species.

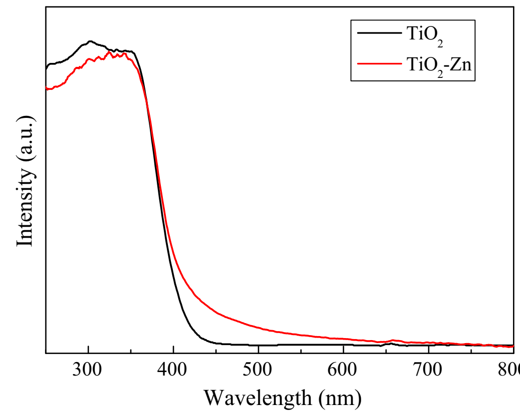

Fig. 4. UV–vis absorption spectra of TiO_2 and TiO_2-Zn.

Under illumination, the electrons can be excited from the valence band to the conduction band of TiO_2. The photo-excited electrons in the conduction band of TiO_2 fall into the oxygen vacancies (defects) via a nonradiative process (τ_1) and then recombine with the holes in the valence band, accompanying with an irradiative process (τ_2). Therefore, the decrease of PL peak intensity and the prolonged life-time of PL decay curve related to irradiative process (τ_2) usually suggest the suppressed recombination of electrons and holes. As shown in Fig. 5A, the pure TiO_2 exhibits a relative high PL intensity, ascribed to the electron transition from the defects to the valence band of TiO_2, suggesting a high recombination rate for TiO_2. Moreover, the life-time related to the nonradiative process (τ_1) and irradiative process (τ_2) can be evaluated by fitting the time resolved PL decay curves via double experimental decay, as shown in Fig. 5B and Table 2. The life time (τ_2) of irradiative process related to the recombination of photo-excited electrons and holes for TiO_2-Zn (2.03 ns) is longer than that pure TiO_2 (1.37 ns). Compared with TiO_2, the prolonged life time for TiO_2-Zn indicates the recombination of electrons and holes are suppressed owing to the formation of O–Zn–Cl species. It is noted that the energy level of oxygen vacancies located at about 0.4 eV and 0.7 eV below the conduction band of TiO_2 [17]. As the energy level of O–Zn–Cl species, which located at about 0.2 eV below the conduction band of TiO_2, is above the energy levels of oxygen vacancies, the excited electrons on the conduction band of TiO_2 would fall into the energy level of surface O–Zn–Cl species other than the oxygen vacancies, suppressing the recombination of electrons and holes effectively. Therefore, according to the discussion above, the existence of surface O–Zn–Cl on the surface of TiO_2 are able to inhibit the recombination of photo-excited charge

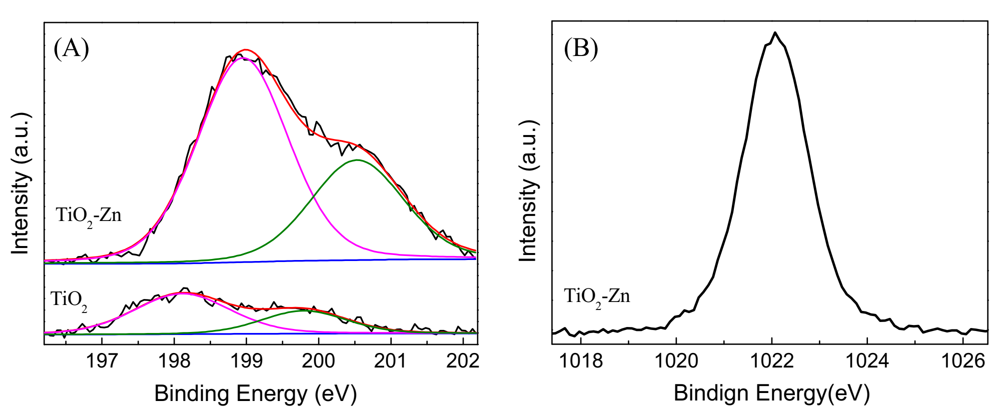

Fig. 3. (A) XPS Cl 2p spectra of TiO_2 and TiO_2-Zn; (B) Zn $2p_{3/2}$ spectra of TiO_2-Zn.

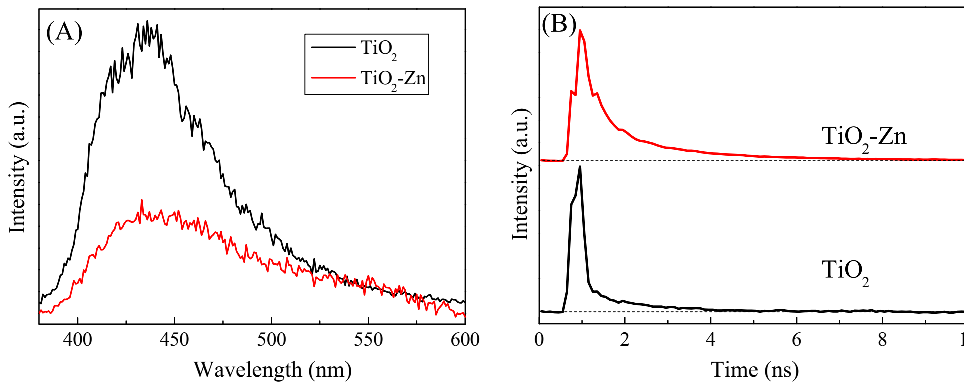

Fig. 5. PL spectra (A) and time-resolved PL decay curve (B) for TiO_2 and TiO_2-Zn sample, excited at 400 nm and monitored at 450 nm.

Table 2
Values of the calculated decay time constant τ_1 and τ_2 via double exponential decay fitting for the corresponding samples.

	TiO_2	TiO_2-Zn
τ_1	0.16 ns	0.47 ns
τ_2	1.37 ns	2.03 ns

carriers and prolong the lifetime of electrons, leading to an improved photocatalytic activity.

The photo-reduction of CO_2 into CH_4 in water with the irradiation of Xenon arc lamp is applied to evaluate the photocatalytic activity of TiO_2 and TiO_2-Zn. CO is the immediate product and CH_4 is the final product. The photocatalytic results are plotted in Fig. 6. Pure TiO_2 exhibit a limited photocatalytic activity and only about 0.350 µmol of CH_4 is produced after 8 hours' irradiation. As we expect, the Zn modified TiO_2 (TiO_2-Zn) exhibit a much better photocatalytic activity and almost 0.851 µmol of CH_4 is detected, which is almost three times as that for pure TiO_2. Hence is can be concluded from the photocatalytic experiment that the introduction of unique surface O–Zn–Cl species is an effective method to improve the photocatalytic activity of TiO_2. The detailed photocatalytic mechanism would be discussed in the following sections.

4. Discussion

According to the discussion above, the photocatalytic mechanism of TiO_2-Zn could be explained via the schematic diagram band structure, as shown in Fig. 7. For pure TiO_2 sample, quite a few electrons and holes can be excited under irradiation and the

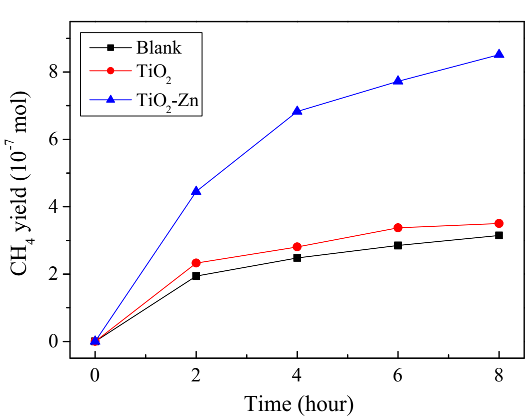

Fig. 6. CH_4 generation over pure TiO_2 and TiO_2-Zn.

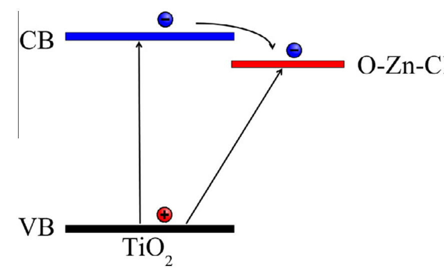

Fig. 7. Scheme of photocatalytic mechanism for TiO_2-Zn under Xenon arc lamp irradiation. The red line indicate the energy level of surface O–Zn–Cl species. (For interpretation of the references to color in this figure legend, the reader is referred to the web version of this article.)

recombination rate of the charge carriers are relatively high, resulting in a poor photocatalytic activity on reduction of CO_2 into CH_4. For TiO_2-Zn, owing to the introduction of O–Zn–Cl surface species, electrons can be excited from the valence band of TiO_2 to the surface energy level of O–Zn–Cl, located at 0.2 eV below the conduction band of TiO_2. At the same time, the electrons on the conduction band of TiO_2 would transfer to energy level of O–Zn–Cl species other than recombine with the holes, suppressing the recombination of electrons and holes. Moreover, the lifetime of photogenerated electrons is also prolonged owing to the surface O–Zn–Cl species. More photogenerated electrons and holes are able to participate in the photocatalytic reaction. The holes in the valence band react with the adsorbed H_2O to form H^+ and oxygen. Meanwhile, the exited electrons would be captured directly by the surface adsorbed CO_2 molecules to form CO and oxygen. The resultant CO would further react with electrons and H^+ to generate the final product, CH_4. Therefore, the TiO_2-Zn sample represents a better photocatalytic activity than pure TiO_2, owing to the formation of O–Zn–Cl species.

5. Conclusions

In summary, unique surface O–Zn–Cl species modified TiO_2 is prepared by a simple sol-gel method. The formation of O–Zn–Cl species would enhance the photocatalytic activity of TiO_2 on photoreduction of CO_2 into CH_4, by extending the absorption into visible region, separating the photogenerated charge carriers and prolonging the lifetime of electrons. It is believed that this work may offer a better understanding about the surface metal-chlorine modified TiO_2 based photocatalysts with improved photocatalytic performance, which can be applied in many fields, such as photo-degradation and photosynthesis.

Acknowledgements

This work is supported by the National Natural Science Foundation of China (Nos. 21173121 and 51372120).

References

[1] S. Sakthivel, H. Kisch, Photocatalytic and photoelectrochemical properties of nitrogen-doped titanium dioxide, ChemPhysChem 4 (2003) 487–490.
[2] T. Lindgren, J.M. Mwabora, E. Avendaño, J. Jonsson, A. Hoel, C.-G. Granqvist, S.-E. Lindquist, Photoelectrochemical and optical properties of nitrogen doped titanium dioxide films prepared by reactive DC magnetron sputtering, J. Phys. Chem. B 107 (2003) 5709–5716.
[3] H. Sato, K. Ono, T. Sasaki, A. Yamagishi, First-principles study of two-dimensional titanium dioxides, J. Phys. Chem. B 107 (2003) 9824–9828.
[4] R. Asahi, T. Morikawa, T. Ohwaki, K. Aoki, Y. Taga, Visible-light photocatalysis in nitrogen-doped titanium oxides, Science 293 (2001) 269–271.
[5] N. Vlachopoulos, P. Liska, J. Augustynski, M. Grätzel, Very efficient visible light energy harvesting and conversion by spectral sensitization of high surface area polycrystalline titanium dioxide films, J. Am. Chem. Soc. 110 (1988) 1216–1220.
[6] P. Zhang, Y. Yu, E. Wang, J. Wang, J. Yao, Y. Cao, Structure of nitrogen and zirconium co-doped titania with enhanced visible-light photocatalytic activity, ACS Appl. Mater. Interfaces 6 (2014) 4622–4629.
[7] J. Wang, Y. Yu, S. Li, L. Guo, E. Wang, Y. Cao, Doping behavior of Zr^{4+} Ions in Zr^{4+}-doped TiO_2 nanoparticles, J. Phys. Chem. C 117 (2013) 27120–27126.
[8] J. Yuan, E. Wang, E. chen, W. Yang, J. Yao, Y. Cao, Doping mode, band structure and photocatalytic mechanism of B-N-codoped TiO_2, Appl. Surf. Sci. 257 (2011) 7335–7342.
[9] S. Sato, R. Nakamura, S. Abe, Visible-light sensitization of TiO_2 photocatalysts by wet-method N doping, Appl. Catal. A 284 (2005) 131–137.
[10] C. Di Valentin, G. Pacchioni, A. Selloni, Theory of carbon doping of titanium dioxide, Chem. Mater. 17 (2005) 6656–6665.
[11] P.G. Wu, C.H. Ma, J.K. Shang, Effects of nitrogen doping on optical properties of TiO_2 thin films, Appl. Phys. A 81 (2004) 1411–1417.
[12] Y. Yu, Y. Tang, J. Yuan, Q. Wu, W. Zheng, Y. Cao, Fabrication of N-TiO_2/$InBO_3$ heterostructures with enhanced visible photocatalytic performance, J. Phys. Chem. C 118 (2014) 13545–13551.
[13] Y. Cao, T. He, Y. Chen, Y. Cao, Fabrication of rutile TiO_2–Sn/anatase TiO_2–N heterostructure and its application in visible-light photocatalysis, J. Phys. Chem. C 114 (2010) 3627–3633.
[14] W. Zhou, H. Liu, J. Wang, D. Liu, G. Du, J. Cui, Ag_2O/TiO_2 nanobelts heterostructure with enhanced ultraviolet and visible photocatalytic activity, ACS Appl. Mater. Interfaces 2 (2010) 2385–2392.
[15] X. Zhang, L. Zhang, T. Xie, D. Wang, Low-temperature synthesis and high visible-light-induced photocatalytic activity of BiOI/TiO_2 heterostructures, J. Phys. Chem. C 113 (2009) 7371–7378.
[16] Y. Yu, E. Wang, J. Yuan, Y. Cao, Enhanced photocatalytic activity of titania with unique surface indium and boron species, Appl. Surf. Sci. 273 (2013) 638–644.
[17] Y. Cao, Y. Yu, P. Zhang, L. Zhang, T. He, Y. Cao, An enhanced visible-light photocatalytic activity of TiO_2 by nitrogen and nickel-chlorine modification, Sep. Purif. Technol. 104 (2013) 256–262.
[18] E. Wang, P. Zhang, Y. Chen, Z. Liu, T. He, Y. Cao, Improved visible-light photocatalytic activity of Titania activated by nitrogen and indium modification, J. Mater. Chem. 22 (2012) 14443–14449.
[19] E. Wang, W. Yang, Y. Cao, Unique surface chemical species on indium doped TiO_2 and their effect on the visible light photocatalytic activity, J. Phys. Chem. C 113 (2009) 20912–20917.
[20] X. Wang, J.C. Yu, Y. Chen, L. Wu, X. Fu, ZrO_2-modified mesoporous nanocrystalline $TiO_{2-x}N_x$ as efficient visible light photocatalysts, Environ. Sci. Technol. 40 (2006) 2369–2374.
[21] S.U. Khan, M. Al-Shahry, W.B. Ingler, Efficient photochemical water splitting by a chemically modified N-TiO_2, Science 297 (2002) 2243–2245.
[22] K.-P. Wang, H. Teng, Zinc-doping in TiO_2 films to enhance electron transport in dye-sensitized solar cells under low-intensity illumination, Phys. Chem. Chem. Phys. 11 (2009) 9489–9496.
[23] J.C. Xu, M. Lu, X.Y. Guo, H.L. Li, Zinc ions surface-doped titanium dioxide nanotubes and its photocatalysis activity for degradation of methyl orange in water, J. Mole. Catal. A – Chem. 226 (2005) 123–127.
[24] W. Li, D. Wu, Y. Yu, P. Zhang, J. Yuan, Y. Cao, Y. Cao, J. Xu, Investigation on a novel ZnO/TiO_2-B photocatalyst with enhanced visible photocatalytic activity, Phys. E: Low-dimensional Syst. Nanostruct. 58 (2014) 118–123.
[25] Y. Yu, J. Wang, W. Li, W. Zheng, Y. Cao, Doping mechanism of Zn^{2+} ions in Zn-doped TiO_2 prepared by a sol–gel method, CrystEngComm 17 (2015) 5074–5080.
[26] H. Zhong, J. Wang, X. Chen, Z. Li, W. Xu, W. Lu, Effect of Mn^+ ion implantation on the Raman spectra of ZnO, J. Appl. Phys. 99 (10) (2006) 3905. 103905–103905–3.